Microstructural Characteristics of High Velocity Oxygen Fuel (HVOF) sprayed NiCrBSi-SiC Composite Coating on a Low Alloy Steel

M.Karagöz[1] , S.Islak[2], S.Buytoz[3], B.Kurt[1]
[1]Bartin University, Faculty of Engineering, Department of Metallurgy and Materials Engineering, 74100 Bartin/Turkey, mkaragoz@bartin.edu.tr
[2]Kastamonu University, Cide Rifat Ilgaz Vocational High School, 37100 Kastamonu, Turkey, sislak@kastamonu.edu.tr
[3]Firat University, Technical Education Faculty, Metal Department, 23100 Elazig, Turkey, sbuytoz@gmail.com

***Abstract*—In this study, NiCrBSi-SiC powders were sprayed using a high velocity oxygen fuel technique on AISI 1030 steel substrate. Powder mixtures with different weight mixing ratios, NiCrBSi+10 wt.% SiC, NiCrBSi+20 wt.% SiC and NiCrBSi+40 wt.% SiC coatings were prepared. The deposited coatings are compared in terms of their phase composition, microstructure and hardness. It is proved that the degree of mixing of the NiCrBSi and SiC components in the powder has massive effect on the phase composition, microstructure and hardness of the coatings. The structure and morphologies of Ni-based coatings were investigated by X-ray diffraction (XRD), scanning electron microscopy (SEM) and energy dispersive spectrometer (EDS) and optical microscope (OM). Microstructures of the coatings have been revealed to the presence of a large amount of dispersed Ni and Cr carbide and/or borides in the Ni matrix. Microhardness of the coatings is found to in the range of 550–830 Hv, which is higher than the substrate material.**

***Keywords*—HVOF, NiCrBSi-based coating, SiC powder**

I. INTRODUCTION

High Velocity Oxygen Fuel (HVOF) is a coating deposition process whereby a powder coating material is heated rapidly in a hot gaseous medium. Simultaneously the powder material is then projected at a high particle velocity onto a prepared substrate surface where it builds up to produce the desired coating. [1]. High Velocity Oxygen Fuel (HVOF) sprayed coatings have been used widely throughout the last decade mainly in industrial applications, aerospace, and power plants, because of the coatings express low porosity and oxide content, high hardness and high adhesion. [2-6]. The main advantage of HVOF compared to other thermal spray techniques is the ability to accelerate the melted powder particles of the feedstock material at a relatively large velocity [7]. The high-velocity oxy-fuel (HVOF) thermal spraying process has shown to be one of the best methods for depositing conventional Ni based and NiCr feedstock powders, because the hypersonic velocity of the flame shortens the time of interaction between the powder and the flame [8,9]. These effects in conjunction with the relatively low temperature (as compared to plasma based techniques) result in less decomposition of the carbide particles during spraying.

Nickel-based alloys are applied extensively in a number of applications both because of their outstanding wear and corrosion resistance at high temperatures and their relatively low cost [10-13]. They have high strength and hardness and good corrosion resistance due to the addition of chromium [14]. Boron brings down the melting temperature and helps in the formation of hard phases. Silicon is added to increase self-fluxing properties. Carbon produces carbides with high hardness levels that improve the wear resistance of coatings [15,16]. Considerable research studies were carried out to examine the HVOF coatings [17-24]. Wear and corrosion resistance of NiCrBSi coating deposited using AC- HVAF technique was investigated by Liu et al. [19]. They determined that the excellent wear properties of the Ni-based coating were tested in a dry sliding wear test. The corrosion resistance of the Ni-based coating founded higher than that of the stainless steel substrate material due to the passive film forming effect of Cr. The hot corrosion behavior of NiCrBSi coatings deposited on Ni- and Fe- based superalloys was investigated by Sidhu et al [20]. They showed that structure of the as sprayed NiCrBSi coating mainly consisted of γ-nickel solid solution containing small fraction of Cr_7C_3, Ni_3B phases and $NiCr_2O_4$ spinel oxides. However, they founded that the hot corrosion resistance imparted by NiCrBSi coatings may be attributed to the formation of oxides of silicon, chromium, nickel and spinels of nickel and chromium in the molten salt environment at 900 °C. The influence of microstructural and mechanical properties and wear resistance of HVOF sprayed WC-Co and WC-Ni coatings were examined by Berger et al. [21]. They founded that the resistance to erosive wear was improved when cobalt was used as binder metal. The influence of spray parameters on the microstructure and mechanical properties of Colmonoy 88 alloy HVOF coating were studied by Sosa et al. [22]. They determined that the microstructure consist of increase in the unmelted particles volume fraction and the development of interlamellar microcracks as the spraying distance increases, leading to a decrease in the elastic modulus of the coatings. The adhesion

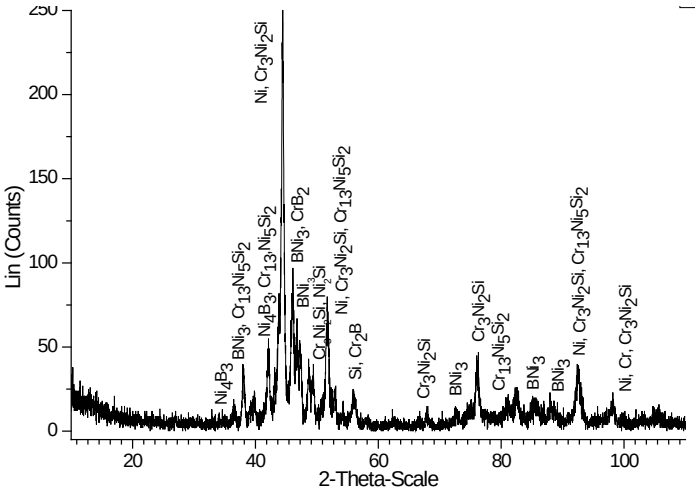
evaluation of different interlayers such as Co–Cr, Ni–Cr (80–20) HVOF (High Velocity Oxy-Fuel) thermally sprayed coatings and Ni-plating between the cermet based WC–Co–Cr coatings were examined by Hadad et al. [23]. They indicated that the electrochemically deposited interlayer Ni-plating provides the highest adhesion to cermet coating within the multilayered structured coatings.

The aim of this work was to prepare Ni-based coatings by the HVOF technique and to study their microstructure and properties. The surface properties, such as microstructure, hardness and porosity of NiCrBSi-SiC coatings prepared by HVOF coating process have been investigated.

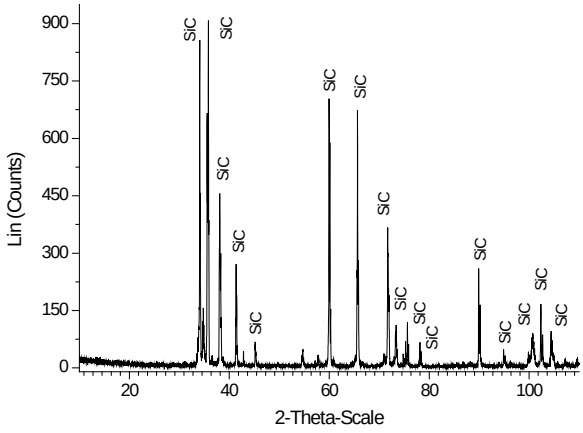
II. EXPERIMENTAL PROCEDURES

A mixture of a NiCrBSi with an average grain size of 60 μm and SiC with an average grain size of 68 μm powder was used as spray material. XRD analysis results of the powders are described in Fig.1a and b**.** From the morphology of the powder given in Fig. 2, NiCrBSi powders can be observed that the powder completely consists of spherical particles (Fig. 2a) while SiC powder revealed the angular shape of the ceramic particles (Fig 2c). The chemical composition of all the materials is summarized in Table 1.

The substrates were pre-cleaned in acetone for 5 min, and then blast-cleaned by 60 mesh aluminum oxides for 5 min to improve the adhesion of the coating onto the substrate. The spraying was carried out with the HIPOJET 2100 HVOF system (Kobatek Surface Treatment Industry Co.Ltd. Istanbul, Turkey). Fig.3 shows the schematic diagram of the coating system. The spraying parameters optimized to produce the coatings on the steel substrate are summarized in Table 2. Propane gas was used as a fuel gas. During spraying, the pressures of the propane and oxygen were fixed at 5 bar and 7 bar, respectively. The flow of oxygen was set to 439 l/min. The flow of the propane was 35 l/min and 45 l/min for NiCrBSi and SiC powders. Nitrogen gas was used as powder feed gas, which was operated at a pressure of 5 bar. The spray distance from the gun exit to the substrate surface was kept at 180-200 mm throughout the spraying process.

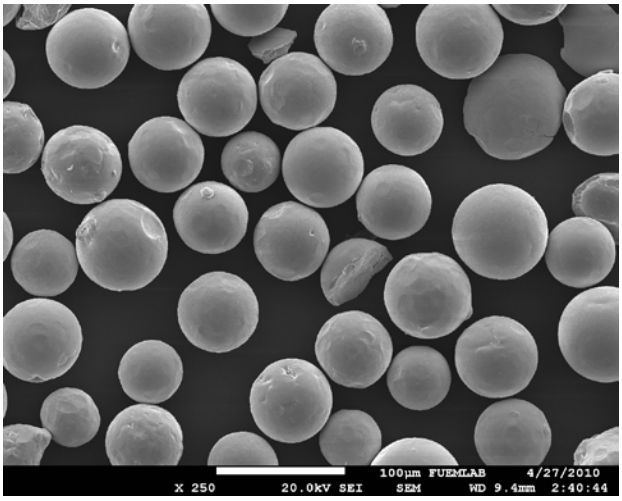


(a)

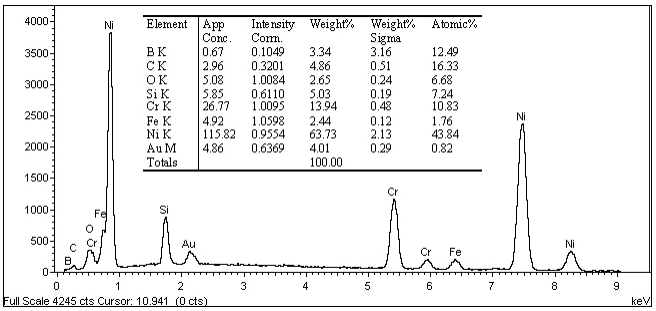


(b)

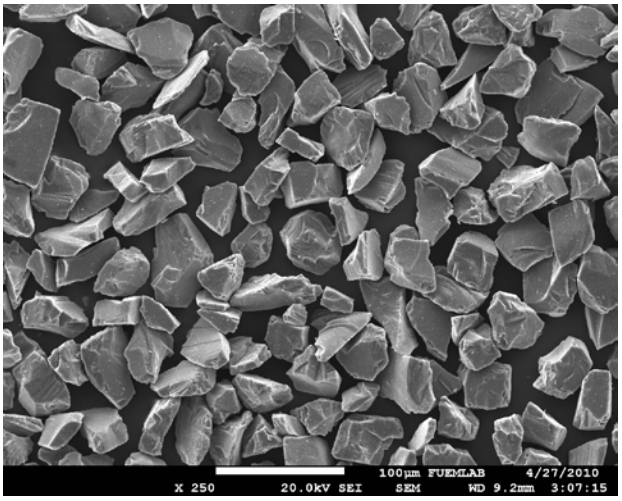
Figure 1: XRD analysis of powders: (a) NiCrBSi and (b) SiC



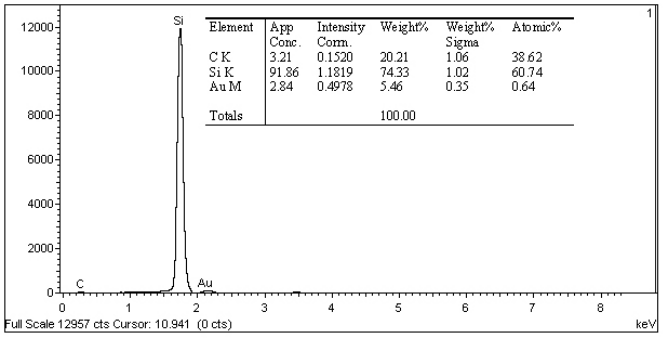
(a)



(b)



(c)



(d)

Figure 2: SEM imagines and EDX spectrums of powders used HVOF spray: (a), (b) NiCrBSi powder, (c) and (d) SiC powder

The coatings studied in this work were NiCrBSi and SiC powders deposited on a steel substrate with a thickness of approximately 250 µm, using a high-velocity oxy-fuel system (HVOF). Three different content NiCrBSi powders were used as feedstock powders in the present investigation, namely (a) 90wt.% NiCrBSi, (b) 80wt.% NiCrBSi and (c) 60wt.% NiCrBSi. The sample codes and coating powders with various SiC content are listed in Table 3.

Table 1: Chemical compositions of AISI 1030 steel, NiCrBSi and SiC powders (wt.%) used for surface coating

	Substrate&Feedstock powders			
		AISI 1030 steel	NiCrBSi powder	SiC powder
Composition (wt.%)	C	0.32	4.86	20.21
	Mn	0.58	-	-
	Si	0.21	5.03	74.33
	Ni	0.45	Balance	-
	Cr	0.095	13.94	-
	Fe	Balance	3.97	-
	B		3.34	-

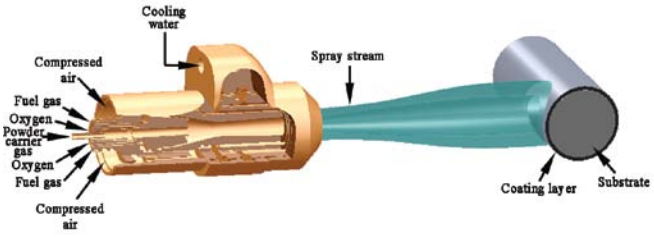


Figure 3: Schematic representation of HVOF system

Coatings were then air-cooled. Samples prepared for metallograpy examinations after coating process were polished with conventional metallograpy processes after mechanical treatments. Samples polished were etched with ferric chloride etching agent (25 g $FeCl_3$+25 ml HCl+100 ml H_2O). For each coating, microstructure and phase were investigated using a scanning electron microscope (SEM) and X-ray diffraction (XRD). Surface hardness was measured using an Instron Wolpert tester with a load of 100 g and a loading time of 10 s, and porosity was determined by analyzing images photographed by an optical microscope.

Table 2: Spraying parameters

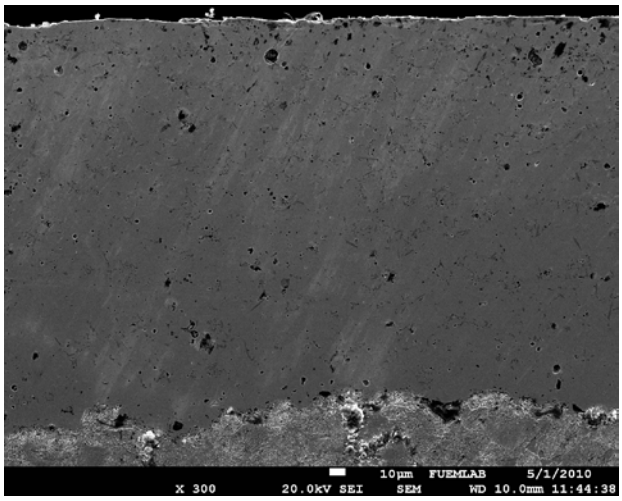
HVOF gun type	HIPOJET 2100
Oxygen gas pressure (bar)	7
Fuel gas (C_3H_8) pressure (bar)	5
Compressed air pressure (bar)	5
Powder feed rate (g/min)	55
Spray distance (mm)	180-200
Gun speed (mm/sec)	3
Carrier gas (N_2) pressure (bar)	5

Table 3: The coating powders with various SiC contents

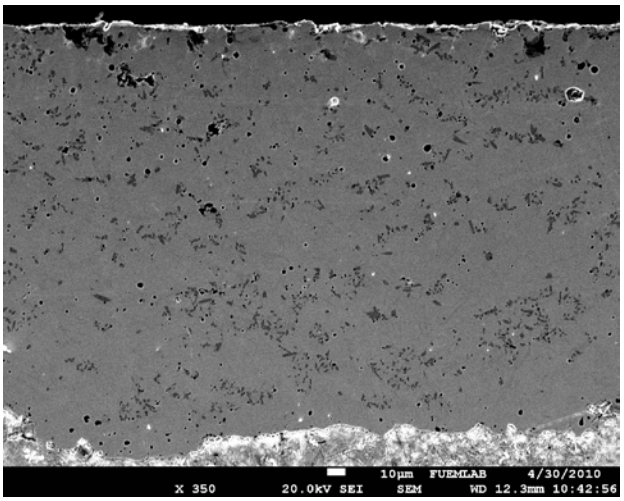
Sample number	**Matrice powder content**	**Reinforcement powder content**
Coating 1	90wt. % NiCrBSi	10wt. % SiC
Coating 2	80wt. % NiCrBSi	20wt.% SiC
Coating 3	60wt. % NiCrBSi	40wt.% SiC

III. Conclusion and discussion

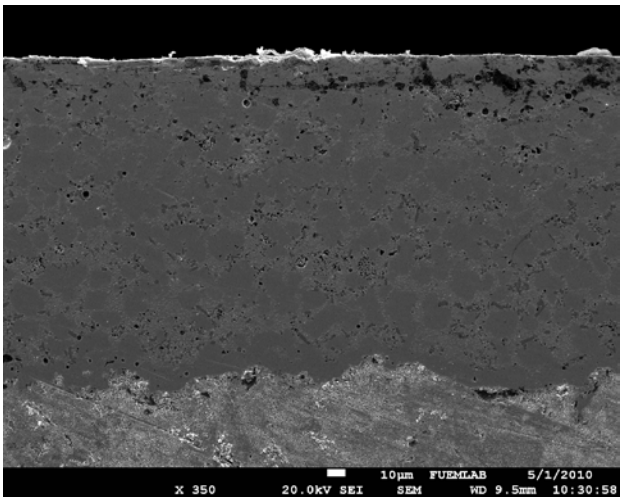
The SEM micrographs at the cross section of HVOF spray coatings are shown in Fig.4 and Fig. 5, respectively. The thickness of the coatings was measured from the micrograph, taken along the cross-section of the mounted samples. All coatings have a thickness of about 250 μm and bond well to the substrate (can be seen in Fig. 4a-c). For the HVOF sprayed nickel-based coating, the typical coating thicknesses are in the range of 250–300 μm as suggested by Sidhu [24]. All coatings were completely crack-free. However, porosity value in the HVOF coatings is low. The microcrystalline HVOF coating shows a very homogeneous microstructure and a porosity of less than 1%. Adherence between substrate and coating seems to be good with a low presence of either cracks or voids in the interface. Porosity is completely eliminated after the fuse process. A low quantity of unmelted particles is shown in Fig 4 (c).



(a)

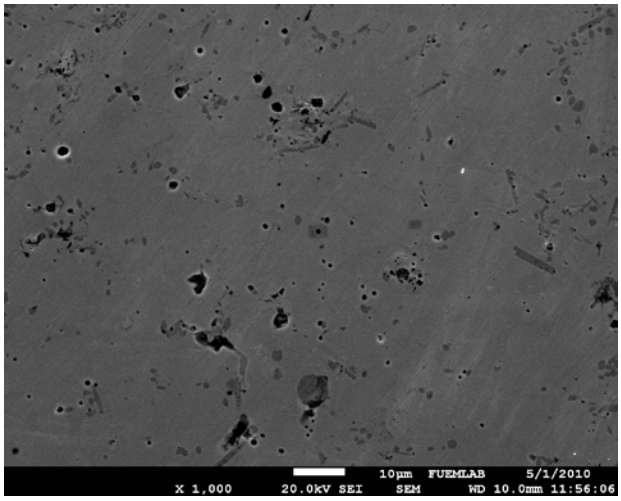


(b)

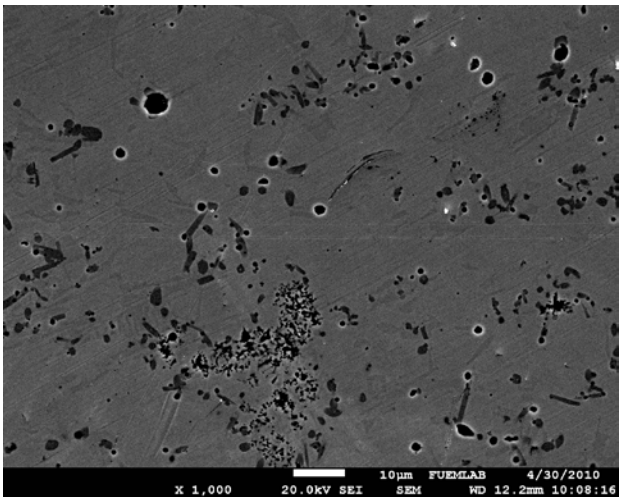


(c)

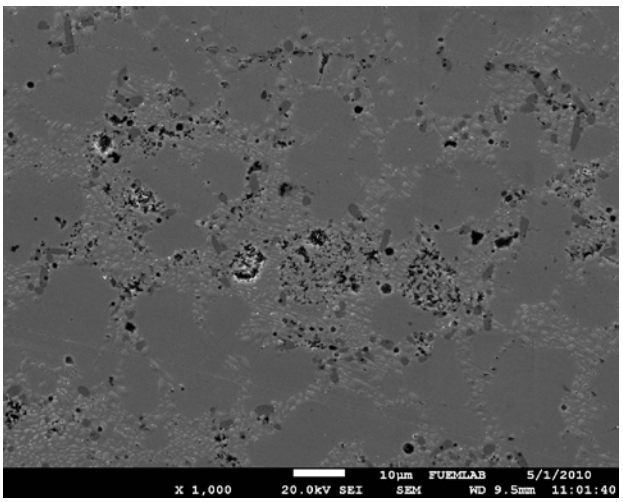
Figure 4: General view of HVOF coatings on low carbon steel: (a), (b) and (c).



(a)



(b)



(c)

Figure 5: SEM imagines showing surface morphology of HVOF sprayed NiCrBSi-SiC coatings on low carbon steel: (a), (b) and (c).

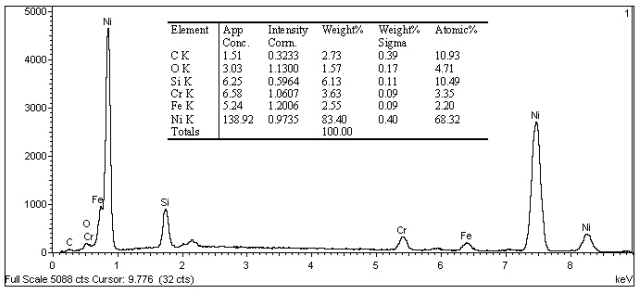
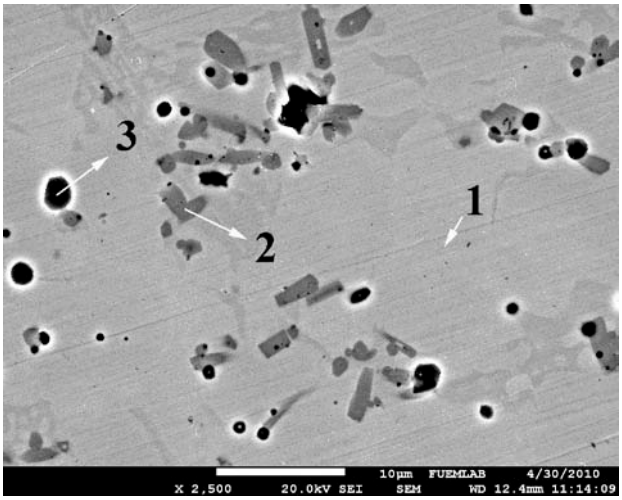
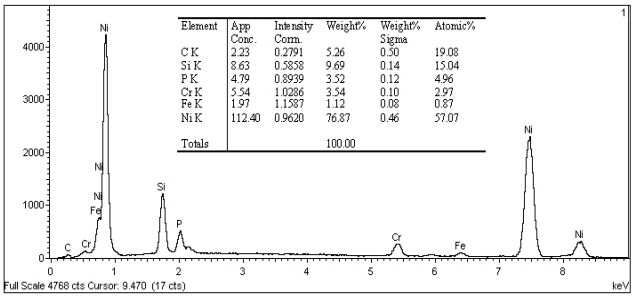


Figure 6: EDS analysis result of the coating 3

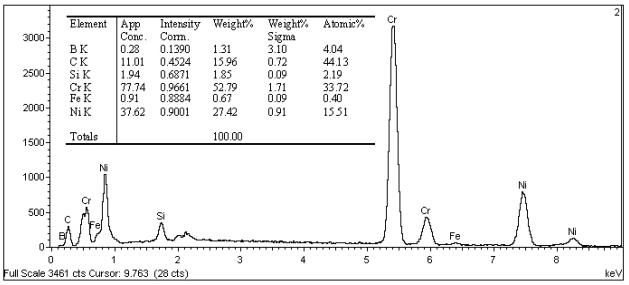
Fig. 5 depicts the SEM micrograph of the surface of the coatings. The coatings have a uniform microstructure (Fig.5a and 5b). Wang and Ohmori [25] study stated that most NiCrBSi particles were completely melted under the present spray conditions. Therefore, the current test results confirm with that HVOF coating deposited with the droplets melted sufficiently will not form effective adhesion to a smooth substrate surface. Some limited porosity is visible as dark contrast spots, but generally the coatings have dense structures (Fig.5b and 5c). Uniform microstructure of the coatings indicates that a high proportion of the feedstock powder appeared to have been fully melted prior to impact on the substrate. In Figure 5c, for the sample-3, the results of EDS analysis of the light grey colored structure which appears intensively in the particle borders are given in Figure 6. According to the analysis results, the structure appearing in the sediment form on the particle borders caused to solidification which contains predominantly C, Cr and Fe in small amounts. The fact that there is oxygen element in small amounts in the structure indicates that the surface has a trend of oxidation. It is resulted from the XRD analysis in Figure 7 that the possibility of Ni_3Si_2, Cr_3Ni_2Si and $Cr_{13}Ni_5Si_2$ phase presence in the structure, which is intensively seen in the particle borders and occurs in the sample labelled with coating-3, is high. Some dark areas appeared in the coating structure or at the coating substrate interface may be the inclusions.



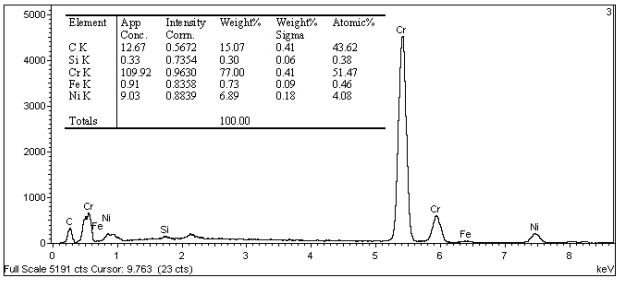
(a)



(b)



(c)



(d)

Figure 7: (a) SEM imagine and EDX results of coating 2 (b) point 1, (c) point 2 and (d) point 3

Image of SEM taken from the sample labelled with coating-2 in high resolution and EDS analysis are also given in Figure

7. As can be seen from Figure 7a, there exist structures based on Ni matrix material, which are randomly scattered and relatively darker grey coloured. This fact is similar in the coating material-3 (Figure 6). In Figure 4b, there are three different structures in SEM microstructure taken from the centre of coating plate with higher magnification (Figure 7a). Based on Ni matrix material, there are structures randomly scattered in, which are relatively dark grey and black. EDS analysis belonging to these structures are given in Figures 7-b, c and d. As the matrix material involves 19.08%C, 15.04%Si, 4.9%P, 2.97%Cr, 0.87%Fe, 57.07%Ni (Figure 7b) in atomic scale, the atomic structure with dark grey colour come to occurrence of solidification with the composition given as follows; 4.04%B, 44.13%C, 2.19%Si, 33.72%Cr, 0.4%Fe, 15.51%Ni (Figure 7c). According to XRD results given in Figure 8, the possibility of the fact that this dark grey coloured structure is CrB_2, Cr_3Ni_2Si and/or Cr_7C_3 is high. The similar findings are achieved by Abdi, Labaili [26] and Planche et. al. [27]. EDS analysis of the dark structure marked with number 3 in Figure 7a is given in Figure 7d. This structure exists in all three samples. The probability of being Cr_7C_3 of this structure is rather high. In case of spraying onto the coating surface, the mixture of NiCrBSi and SiC coating powder decomposes due to high temperature, then forms new phases by re-solidifying during the fusing to the base material. For the structure to be Cr_7C_3 is comply with the XRD results given in Figure 8.

Fig. 8 shows the XRD patterns for the HVOF sprayed NiCrBSi-SiC coatings and it is evident that the coatings mainly consists of γ-nickel based fcc structure as a principal phase. This situation is a feature common in all the nickel-based coated [19,28]. XRD patterns of the coatings have also revealed the presence of very low intensity peaks of Ni_4B_3, BNi_2, BNi_3, SiC and Cr_7C_3 phases. Furthermore, very weak peaks, indexed as belonging to Cr_3Ni_2Si, $Cr_{13}Ni_5Si_2$ and CrB_2 are identified.

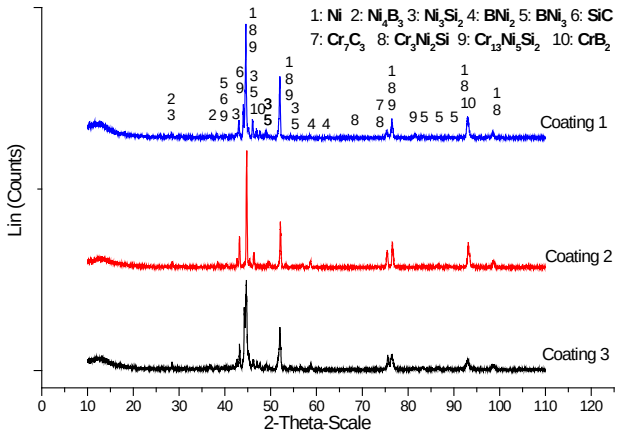
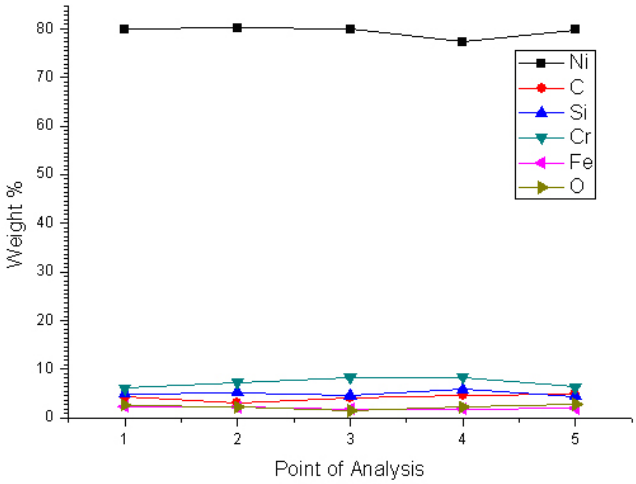
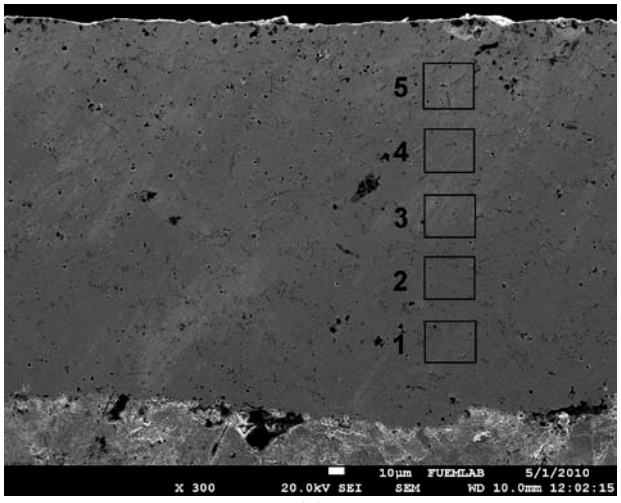


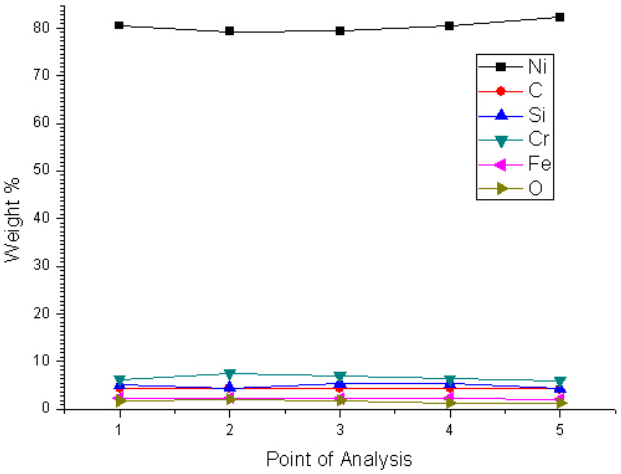
Figure 8: X-ray diffraction for the as sprayed NiCrBSi-SiC coatings on low alloy steel: (a) NiCrBSi-10%SiC, (b) NiCrBSi-20%SiC, (c) NiCrBSi-40%SiC.

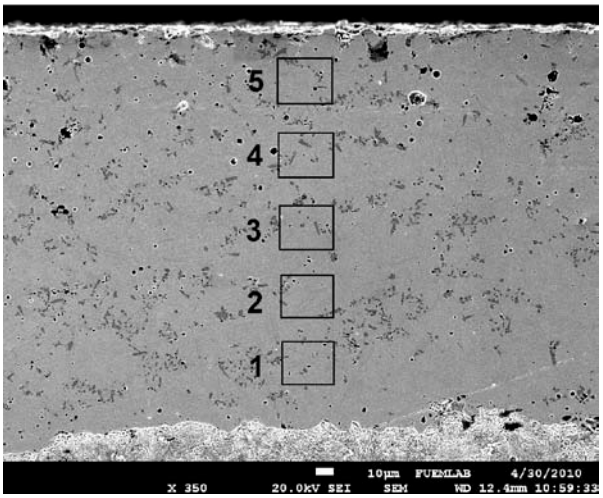
SEM imagines and elemental variation across the cross-section of HVOF coated materials are shown in Fig 9. EDAX analysis of coating 1 (Fig. 9a) reveals that the concentration of Ni, Cr and C decreases at point 1, whereas at points 2, 3 and 4 amounts of Cr is relatively more. Quantity of Ni only increased at point 2, but this element is at its minimal value at the point 4. EDAX analysis of coating 2 (Fig. 9b) shows that the Ni and C elements are almost remained constant at point 1 to 5. Although quantity of Cr is higher at point 3, the concentration of Cr is the lowest at point 5. As Fig. 9c reveals, for EDAX analysis results of coating 3, the weight percentage of Si, C and O_2 increases at point 5 where Ni decreases substantially signifying that dark contrast phase at the top of scale might be rich with oxides of Cr, C and Si. The existence of higher oxygen at point 5 might lead to the formation of Cr- and Si-rich oxide scale. Dark black phase present at the upper of the coating (point 5) which is found to be rich with Si and C is un-melted of SiC particles. It is believed that SiC grains might be retained due to inadequate time to find for the deposition and re-solidification of molten or semi-molten droplets. Both XRD analysis results (can be seen in Fig.8) and EDAX analysis results (can be seen in Fig. 7 and Fig. 9) reveals that the major phase of NiCrBSi-SiC coating is austenite structure rich with Ni, Cr, C and Si.



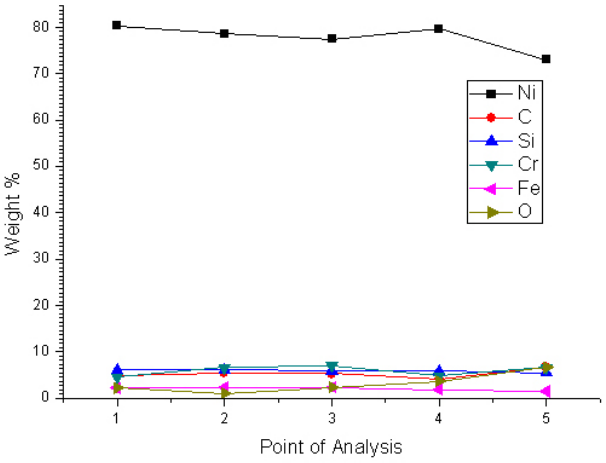


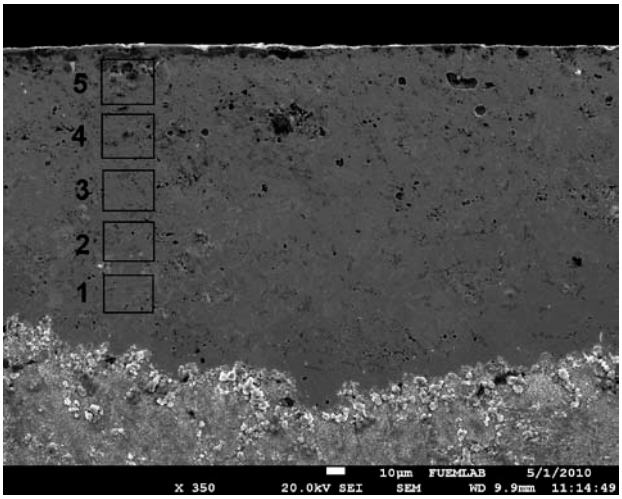
(a)





(b)

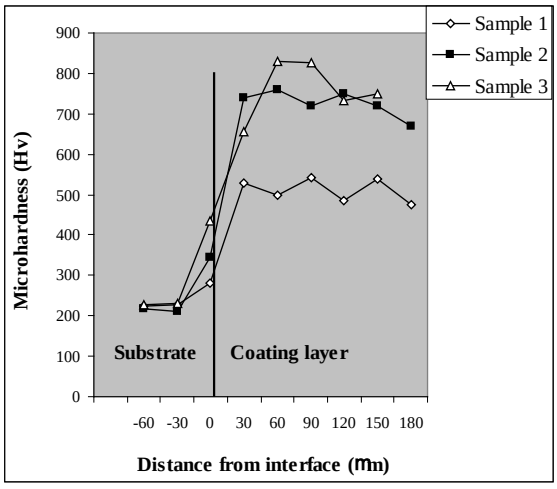




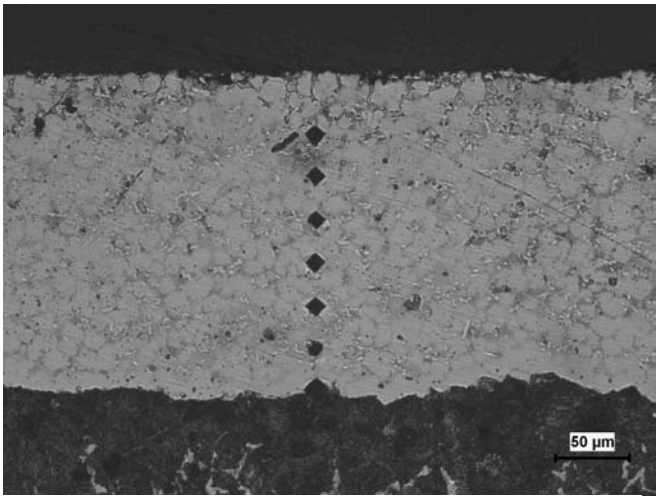
(c)

Figure 9: SEM imagines and variations of elemental composition across the cross-section of HVOF coated with NiCrBSi and SiC mixed powders: (a) coating 1, (b) coating 2 and (c) coating 3.

The microhardness data of the coatings are shown in Fig. 10a, which shows the microhardness profiles along the cross section of the coatings as a function of distance from the coating-substrate interface (Fig. 10b). The microhardness of the substrate is in the range of 210–230 Hv. The microhardness of the coatings is found to be variable with the distance from the coating–substrate interface. This significant variation in the microhardness along the thickness of the coatings might be due to the distribution of the SiC hard phase in Ni-based alloy matrix. Maximum value of about 831 Hv was obtained from the coating 3, while sample 1 showed minimum values of about 474 Hv. Microhardness of the coating for coating 2 is found in the range of 750 Hv. Further, an increase in microhardness of all the substrates was observed near the coating–substrate interface.



(a)



(b)

Figure 10: Microhardness profiles for HVOF sprayed NiCrBSi-SiC coatings on the low alloy steel

IV. CONCLUSIONS

1. Under the employed spray conditions, NiCrBSi and SiC mixed powders have been successfully deposited by HVOF process to develop coatings of average 250 µm thick on AISI 1030 steel substrates. Microhardness of the coatings is found to in the range of 550–830 Hv, which is higher than the substrate material.

2. The microstructure of the as sprayed coating has a nickel based fcc structure as the principal phase. XRD analysis of the coating microstructures revealed the presence of low intensity peaks of Ni_4B_3, BNi_2, BNi_3, SiC and Cr_7C_3 phases. Furthermore, very weak peaks, indexed as belonging to Cr_3Ni_2Si, $Cr_{13}Ni_5Si_2$ and CrB_2 are identified.

ACKNOWLEDGMENT

The authors would like to thank Mr. Rakim Tuncer of KOBATEK Surface Treatment Industry Company of Turkey for performing HVOF.

REFERENCES

[1] M. Hasan, J. Stokes, L. Looney, M.S.J. Hashmi, Effect of spray parameters on residual stress build-up of HVOF sprayed aluminium/tool-steel functionally graded coatings, Surface and Coatings Technology, 202 16 (2008) 4006-4010.

[2] W. Fang, T.Y. Cho, J.H. Yoon, K.O. Song, S.K. Hur, S.J. Youn, H.G. Chun, Processing optimization, surface properties and wear behavior of HVOF spraying WC–CrC–Ni coating, Journal of Materials Processing Technology, 209 7 (2009) 3561-3567

[3] Z. Zhou, L. Wang, F.C. Wang, H.F. Zhang, Y.B. Liu, S.H. Xu, Formation and corrosion behavior of Fe-based amorphous metallic coatings by HVOF thermal spraying, Surface and Coatings Technology, 204 5 (2009) 563-570

[4] O. Culha, E. Celik, N.F. Ak Azem, I. Birlik, M. Toparli, A. Turk, Microstructural, thermal and mechanical properties of HVOF sprayed Ni–Al-based bond coatings on stainless steel substrate, Journal of Materials Processing Technology, 204 1-3 (2008) 221-230.

[5] Hanbey Hazar, Characterization of MoN coatings for pistons in a diesel engine, Materials & Design, 31-1 (2010) 624-627.

[6] Shi-Hong Zhang, Tong-Yul Cho, Jae-Hong Yoon, Ming-Xi Li, P.W. Shum, Sik-Chol Kwon, Investigation on microstructure, surface properties and anti-wear performance of HVOF sprayed WC–CrC–Ni coatings modified by laser heat treatment, Materials Science and Engineering: B, 162 2 (2009) 127-134.

[7] Tahar Sahraoui, Sofiane Guessasma, M. Ali Jeridane, Mohamed Hadji, HVOF sprayed WC–Co coatings: Microstructure, mechanical properties and friction moment prediction, Materials & Design, 31 3 (2010) 1431-1437.

[8] J.A. Picas, A. Fornand, G. Matthäus, HVOF coatings as an alternative to hard chrome for pistons and valves, Wear, 261 5-6 (2006) 477-484.

[9] E.J. Carrasquero, J. Lesage, E.S. Puchi-Cabrera, M.H. Staia, Fretting wear of HVOF Ni–Cr based alloy deposited on SAE 1045 steel, Surface and Coatings Technology, 202 18 (2008) 4544-4551.

[10] C. Navas, R. Colaço, J. de Damborenea, R. Vilar, Abrasive wear behaviour of laser clad and flame sprayed-melted NiCrBSi coatings, Surface and Coatings Technology, 200 24 (2006) 6854-6862.

[11] Xinhong Wang, Min Zhang, Zengda Zou, Shiyao Qu, Microstructure and properties of laser clad TiC+NiCrBSi+rare earth composite coatings, Surface and Coatings Technology, 161 2-3 (2002) 195-199.

[12] R. González, M.A. García, I. Peñuelas, M. Cadenas, Ma. del Rocío Fernández, A. Hernández Battez, D. Felgueroso, Microstructural study of NiCrBSi coatings obtained by different processes, Wear, 263 1-6 (2007) 619-624.

[13] M.C. Lin, L.S. Chang, H.C. Lin, C.H. Yang, K.M. Lin, A study of high-speed slurry erosion of NiCrBSi thermal-sprayed coating, Surface and Coatings Technology, 201 6 (2006) 3193-3198.

[14] W. L. Mankins, S. Lamb (Eds.), Nickel and Nickel Alloys, ASM Handbook, vol. 2, ASM International, (1992) 1362-1404.

[15] J. M. Miguel, J. M. Guilemany, S. Vizcaino, Tribological study of NiCrBSi coating obtained by different process, Tribology International, 36 3 (2003) 181-187.

[16] T. Gómez-del Río, M.A. Garrido, J.E. Fernández, M. Cadenas, J. Rodríguez, Influence of the deposition techniques on the mechanical properties and microstructure of NiCrBSi coatings, Journal of Materials Processing Technology, 204 1-3 (2008) 304-312.

[17] T.S. Sidhu, S. Prakash, R.D. Agrawal, Characterisation of NiCr wire coatings on Ni- and Fe-based superalloys by the HVOF process, Surface and Coatings Technology, 200 18-19 (2006) 5542-5549.

[18] M. Gaona, R.S. Lima, B.R. Marple, Influence of particle temperature and velocity on the microstructure and mechanical behaviour of high velocity oxy-fuel (HVOF) -sprayed nanostructured titania coatings, Journal of Materials Processing Technology, 198 1-3 (2008) 426-435.

[19] Shenglin Liu, Xueping Zheng, Gangqiang Geng, Dry sliding wear behavior and corrosion resistance of NiCrBSi coating deposited by activated combustion-high velocity air fuel spray process, Materials & Design, 31 2 (2010) 913-917.

[20] T.S. Sidhu, S. Prakash, R.D. Agrawal, Characterisations of HVOF sprayed NiCrBSi coatings on Ni- and Fe-based superalloys and evaluation of cyclic oxidation behaviour of some Ni-based superalloys in molten salt environment, Thin Solid Films, 515 1 (2006) 95-105.

[21] L.-M. Berger, S. Saaro, T. Naumann, M. Wiener, V. Weihnacht, S. Thiele, J. Suchánek, Microstructure and properties of HVOF-sprayed chromium alloyed WC–Co and WC–Ni coatings, Surface and Coatings Technology, 202 18 (2008) 4417-4421.

[22] J.G. La Barbera-Sosa, Y.Y. Santana, C. Villalobos-Gutiérrez, S. Cabello-Sequera, M.H. Staia, E.S. Puchi-Cabrera, Effect of spray distance on the corrosion-fatigue behavior of a medium-carbon steel coated with a Colmonoy 88 alloy deposited by HVOF thermal spray, Surface and Coatings Technology, In Press, Corrected Proof, Available online 1 February 2010.

[23] M. Hadad, R. Hitzek, P. Buergler, L. Rohr, S. Siegmann, Wear performance of sandwich structured WC–Co–Cr thermally sprayed coatings using different intermediate layers, Wear, 263 1-6 (2007) 691-699.

[24] T.S. Sidhu, S. Prakash, R.D. Agrawal, Studies of the metallurgical and mechanical properties of high velocity oxy-fuel sprayed stellite-6 coatings on Ni- and Fe-based superalloys, Surface and Coatings Technology, 201 1-2 (2006) 273-281.

[25] Y.-Y. Wang, C.-J. Li, A. Ohmori, Examination of factors influencing the bond strength of high velocity oxy-fuel sprayed coatings, Surface and Coatings Technology, 200 9 (2006) 2923-2928.

[26] S. Abdi and S. Lebaili, Alternative to chromium, a hard alloy powder NiCrBCSi (Fe) coatings thermally sprayed on 60CrMn4 steel. Phase and comportements, Physics Procedia 2 (2009) 1005-1014.

[27] M.P. Planche, H. Liao, B. Normand, C. Coddet, Relationships between NiCrBSi particle characteristics and corresponding coating properties using different thermal spraying processes, Surface and Coatings Technology, 200 7 (2005) 2465-2473.

[28] D. Chaliampalias, G. Vourlias, E. Pavlidou, S. Skolianos, K. Chrissafis, G. Stergioudis, Comparative examination of the microstructure and high temperature oxidation performance of NiCrBSi flame sprayed and pack cementation coatings, Applied Surface Science, 255 6 (2009) 3605-3612.